Copyright © 2013 Tech Science Press CMES, vol.93, no.5, pp.363-376, 2013

Three-dimensional Fluid Flow Simulations Using GPU-based Particle Method

K. Kakuda[1], T. Nagashima[1], Y. Hayashi[1], S. Obara[1], J. Toyotani[1], S. Miura[2], N. Katsurada[3], S. Higuchi[3] and S. Matsuda[3]

Abstract: The application of a GPU-based particle method to three-dimensional incompressible viscous fluid flow problems is presented. The particle approach is based on the MPS (Moving Particle Semi-implicit) scheme using logarithmic weighting function to stabilize the spurious oscillatory solutions for solving the Poisson equation with respect to the pressure fields by using GPU-based SCG (Scaled Conjugate Gradient) method. Numerical results demonstrate the workability and the validity of the present approach through the dam-breaking flow problem and flow behavior in a liquid ring pump with rotating impeller blades.

Keywords: GPU-based particle method, MPS, logarithmic weighting function, GPU-based SCG, dam-breaking flow, liquid ring pump, rotating impeller.

1 Introduction

The numerical simulations of three-dimensional (3D) viscous fluid flows including multi-scale/physics and moving boundary/obstacle are indispensable in the fields of engineering and science from a practical point of view. The numerical fluid flow simulations have been successfully performed by many researchers with the use of finite difference method and finite element method [Stein, Borst and Hughes (2004)]. Numerical difficulties have been experienced in the solution of incompressible Navier-Stokes equations at higher Reynolds numbers. Especially, it is well known that the centered finite difference and standard Galerkin finite element formulations lead to spurious oscillatory solutions for flow problem at high Reynolds number regimes. To overcome such spurious oscillations, various upwind/ upstream-based schemes have been consistently presented in both frameworks.

[1] College of Industrial Technology, Nihon University, Narashino, Chiba 275-8575, Japan
[2] Tokyo Metropolitan College of Industrial Technology, Shinagawa-ku, Tokyo 140-0011, Japan
[3] Product Engineering Department, Tsurumi Manufacturing Co., LTD., Tsurumi Tsurumi-ku, Osaka 538-8585, Japan

There are also various gridless/ meshless-based particle methods, such as SPH (Smoothed Particle Hydrodynamics) method [Lucy (1977); Gingold and Monaghan (1977)], MPS (Moving Particle Semi-implicit) method [Koshizuka and Oka (1996)], and MLPG (Meshless Local Petrov-Galerkin) one [Atluri and Zhu (1998); Lin and Atluri (2001); Avila and Atluri (2009); Avila, Han and Atluri (2011)], to simulate effectively such complicated problems. The SPH methods for solving compressible fluid flows with gravity have been firstly developed in the field of astrophysics [Lucy (1977);Gingold and Monaghan (1977)], and applied successfully to a wide variety of complicated physical problems. The MPS method [Koshizuka and Oka (1996)] as an incompressible fluid flow solver has been widely applied to the problem of breaking wave with large deformation, the fluid-structure interaction problem, and so forth. However, the standard/original MPS approach leads to the above-mentioned unphysical numerical oscillation of pressure fields which are described by the discretized Poisson equation. To improve some shortcomings of the standard MPS method, Khayyer and Gotoh have proposed the modified MPS method for the prediction of wave impact pressure on a coastal structure to ensure more exact momentum conservation [Khayyer and Gotoh (2009)]. The improvement of stability in the standard MPS method has been more recently achieved by adding some source terms into Poisson pressure equation [Kondo and Koshizuka (2011)]. Atluri and Zhu [Atluri and Zhu (1998)] have developed the MLPG approach based on the local symmetric weak form and the moving least squares for solving accurately potential problems, and the approach was extended to deal with the problems for incompressible Navier-Stokes equations [Lin and Atluri (2001)] in fluid dynamics. Avila and Atluri [Avila and Atluri (2009)] have presented efficiently various numerical solutions of the non-steady, two-dimensional Navier-Stokes equations by using the MLPG method coupled with a fully implicit pressure-correction approach. They have also proposed a novel MLPG-mixed finite volume method for solving the steady-state Stokes flow involving complex phenomena between eccentric rotating cylinders [Avila, Han and Atluri (2011)].

Recently, the physics-based computer simulations on the GPU (Graphics Processing Units) have increasingly become an important strategy for solving efficiently various problems, such as fluid dynamics [Harris (2004); Crane, Llamas and Tariq (2008); Harada, Masaie, Koshizuka and Kawaguchi (2008); Hori, Gotoh, Ikari and Khayyer (2011)], rigid body dynamics [Harada (2008)], and so forth. In our previous work, we have presented a GPU-based particle scheme using logarithmic weighting function for solving effectively two-dimensional problems of incompressible fluid flow [Kakuda, Nagashima, Hayashi, Obara, Toyotani, Katsurada, Higuchi and Matsuda (2012)]. The GPU-implementation consisted mainly of the five steps, namely, the search for neighboring particles in the influence area, the calculation of the particle number density, solving the Poisson equation with respect to the pressure fields, the calculation of the pressure gradient, and the modification of velocities and positions of the particles. We obtained that the performance on GPU with about $120,000$ particles led to approximately 12 times speed-up.

The purpose of this paper is to present the application of the GPU-based particle method using logarithmic weighting function to 3D incompressible viscous fluid flow problems, namely the dam-breaking flow problem [Martin and Moyce (1952); Hirt and Nichols (1981); Ramaswamy and Kawahara (1987)] and flow in a liquid ring pump with rotating impeller [Kakuda, Ushiyama, Obara, Toyotani, Matsuda, Tanaka and Katagiri (2010)]. The dam-breaking flow problem has been used widely to verify the applicability and validity of the numerical methods. On the other hand, the phenomena in the liquid ring pump require the multi-physics, namely fluid-structure interaction problems [Du and Shen (2010)], including the moving interface boundary between gas and liquid, and also the rotating impeller with blades. The pump has an impeller with blades attached to a center hub, located by the decentering in a cylindrical body [Avila, Han and Atluri (2011)]. The workability and validity of the present approach are demonstrated through the dam-breaking flow problem and flow in the liquid ring pump, and compared with experimental data and other numerical ones.

Throughout this paper, the summation convention on repeated indices is employed. A comma following a variable is used to denote partial differentiation with respect to the spatial variable.

2 Statement of the problem

Let Ω be a bounded domain in 3D Euclidean space with a piecewise smooth boundary Γ. The unit outward normal vector to Γ is denoted by $\boldsymbol{n}$. Also, $\Im$ denotes a closed time interval.

The motion of an incompressible viscous fluid flow is governed by the following Navier-Stokes equations :

$$\frac{Du_i}{Dt} = -\frac{1}{\rho}p_{,i} + \nu u_{i,jj} + f_i \qquad in\ \Im \times \Omega \tag{1}$$

$$\frac{D\rho}{Dt} = 0 \qquad in\ \Im \times \Omega \tag{2}$$

where u_i is the velocity vector component, ρ is the density, p is the pressure, f_i is the external force, ν is the kinematic viscosity, and D/Dt denotes the Lagrangian differentiation.

In addition to Eq. 1 and Eq. 2, we prescribe the initial condition $u_i(\boldsymbol{x},0) = u_i^0$, where u_i^0 denotes the given initial velocity, and the Dirichlet and Neumann boundary conditions.

3 MPS formulation using a logarithmic-type weighting function

The particle interaction models of the MPS as illustrated in Fig. 1(a) are prepared with respect to differential operators, namely, gradient, divergence and Laplacian [Koshizuka and Oka (1996)]. The incompressible viscous fluid flow is calculated by a semi-implicit algorithm, such as SMAC (Simplified MAC) scheme [Amsden and Harlow (1970)]. For the standard MPS formulation, the selection of a weighting function is a key factor in the particle-based framework. If the distance r between the coordinates $\boldsymbol{r}_i$ and $\boldsymbol{r}_j$ is close, then there is a possibility that the computation fails suddenly with unphysical numerical oscillations. Therefore, in order to stabilize such spurious oscillations generated by the standard MPS strategy, we adopt the following logarithmic-type weighting function as shown in Fig. 1(b), and also consider the reduction of *ad hoc* influence radius, r_e, for solving the pressure fields [Kakuda, Nagashima, Hayashi, Obara, Toyotani, Katsurada, Higuchi and Matsuda (2012)]. As a reason for the consideration, the finite element approach is successful only if the pressure field is interpolated with functions at least one order lower than those of the velocity vector field.

$$w(r) = \begin{cases} log(\frac{r_e}{r}) & (r < r_e) \\ 0 & (r \geq r_e) \end{cases} \tag{3}$$

The logarithmic-type weighting function is generally similar to the profile of the weighting function proposed by Kondo and Koshizuka to stabilize the pressure calculations [Kondo and Koshizuka (2011)](see Fig. 1(b)).

The particle number density n at particle i with the neighboring particles j is defined as

$$< n >_i = \sum_{j \neq i} w(|\boldsymbol{r}_j - \boldsymbol{r}_i|) \tag{4}$$

The Poisson equation for solving implicitly the pressure field at particle i is also given as follows [Kondo and Koshizuka (2011)]:

$$\begin{aligned} \frac{1}{\rho_0} < \boldsymbol{\nabla}^2 p >_i = & - \frac{1-\beta}{\Delta t^2} \frac{< n^* >_i - 2 < n^k >_i + < n^{k-1} >_i}{n^0} \\ & - \frac{\beta - \gamma}{\Delta t^2} \frac{< n^* >_i - < n^k >_i}{n^0} - \frac{\gamma}{\Delta t^2} \frac{< n^* >_i - n^0}{n^0} \end{aligned} \tag{5}$$

where ρ_0 is the density in the initial state, $< n^* >_i$ is an auxiliary particle number at particle i, and β and γ denotes the adequate dimensionless parameters.

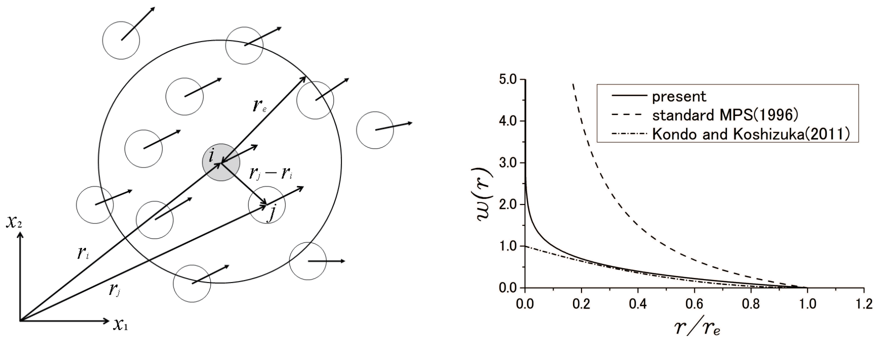

(a) Particle interaction models (2D) (b) Profiles of weighting functions

Figure 1: Particle interaction models and weighting functions

4 GPU implementation using CUDA

The specification of CPU and GPU using CUDA is summarized in Tab. 1. A physical value at particle position is calculated as a weighted sum of the values of neighboring particles in the influence area. Therefore, we have to search for neighboring particles. The difficulty in implementing MPS on the GPU is that the neighborhood relationship among particles dynamically changes during the simulation.

The GPU implementation consists mainly of the following five steps [Kakuda, Nagashima, Hayashi, Obara, Toyotani, Katsurada, Higuchi and Matsuda (2012)]:
1) search for neighboring particles in the influence area;
2) calculation of the particle number density;
3) solving the Poisson equation with respect to the pressure fields by using GPU-based SCG method;
4) calculation of the pressure gradient;
5) modification of velocities and positions of the particles.

5 Numerical examples

In this section we present numerical results obtained from applications of the above-mentioned numerical method to incompressible viscous fluid flow problems, namely dam-breaking flow problem involving free surface and flow in a liquid ring pump with rotating impeller blades from a practical point of view. The initial velocities

Table 1: A summary of the specification of CPU and GPU

CPU	Intel Core i7, 3.50GHz
Memory	DDR3 PC3-10600 16GB
OS	Cent OS 6.0 64bit
Bus	PCI Express 2.0x16
GPU	NVIDIA GeForce GTX580
Global Memory	1.5GB
Processor Clock	1544MHz
Streaming Multiprocessor (SM)	16
CUDA core	512
Memory Transfer Rate	192.4GB/s
Memory Interface	384bit
CUDA Driver	Version 4.10
Tool kit & SDK	Version 4.0

are assumed to be zero everywhere in the interior domain. In three-dimensional simulation, we set the CFL condition $u_{max}\Delta t/l_{min} \leq C$, where C is the Courant number. The kernel sizes for the particle number density and the gradient/Laplacian models are $r_e = 4.0l_0$ and $\bar{r}_e = 2.0l_0$ for velocity and pressure calculations, respectively, in which l_0 is the distance between two neighboring particles in the initial state. In both cases, we set $l_0 = 0.008m$ and also $(\beta, \gamma) = (0.5, 0.05)$.

5.1 Dam-breaking flow problem

Let us first consider the dam-breaking flow problem involving free surface and gravity. Fig. 2 shows the geometry and the initial state of particles $199,540$ for flow in the dam-breaking problem.

The comparisons of CPU and GPU particle-based simulations at each time are shown in Fig. 3, and the agreement between these results appears satisfactory. Fig. 4 shows the accelerating performance of GPU to the CPU time, and also the time evolutions of the leading-edge of the water using the present approach and the standard MPS method through comparison with experimental data [Martin and Moyce (1952)]. We can see from Fig. 4 that the performance with about $199,540$ particles leads to approximately 17.33 times speed-up. The agreement between the present results and the experimental data appears also satisfactory.

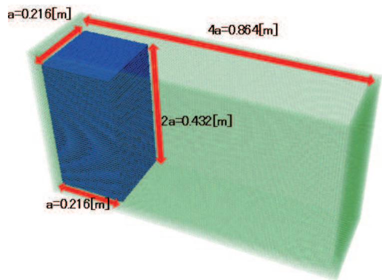

(a) Geometrical configuration

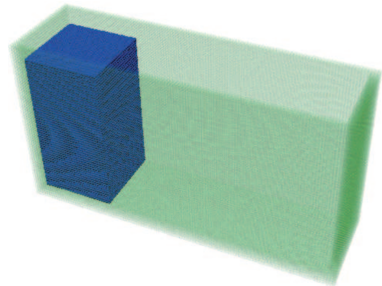

(b) Initial state of particles

Figure 2: Dam-breaking flow problem

5.2 Flow in a liquid ring pump

As the second example, Fig. 5 shows the geometrical configuration and the initial state of particles for flow in a liquid ring pump with rotating impeller. The phenomena in the pump require the multi-physics problem including the moving interface boundary between gas and liquid, and the rotating impeller with blades. In Fig. 5(a) the blades near the top of the pump are very closer to the outside wall than at the side and bottom of the pump. The impeller with blades is attached to a center hub and located in off-set from the center of the cylindrical body. The eccentricity ratio is about 0.387. In this 3D simulation, we set $211,212$ particles in the initial configuration and $2,400$rpm as the speed of the rotating impeller.

Fig. 6 shows the instantaneous particle behaviors for the rotational speed $2,400$rpm of the impeller blades. When the pump starts, the impeller slings the water sealant by centrifugal force, to the outside walls of the body, forming a water ring in the area of impeller blades with passage in the time. As you can see in these figures, some of the blades are fully immersed in water, and some are almost out of the water because of the decentering impeller in the body. The corresponding instantaneous velocity vector fields at different time are shown in Fig. 7. With passage in the time, you can see the extension of high velocity vector fields near the bottom wall of the body. The pump with an impeller of the high rotating speed expands also the high velocity vector field to the neighborhood of the outside wall. Fig. 8 shows also the pressure fields, which is averaged over the time interval from 200*ms* to 400*ms*. We can obtain the maximum value of the pressure field in the upper right, namely, about 315°.

Fig. 9 shows the 2D-simulation (see Fig. 9(a)) and 3D-simulation (see Fig. 9(b)) by using the present approach through comparison with experimental photograph (see

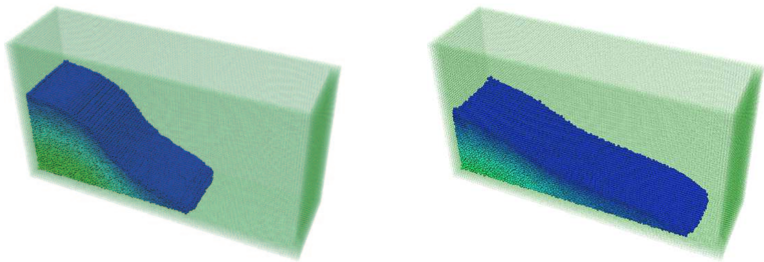

(a.1) $t \approx 0.21s$ (a.2) $t \approx 0.30s$

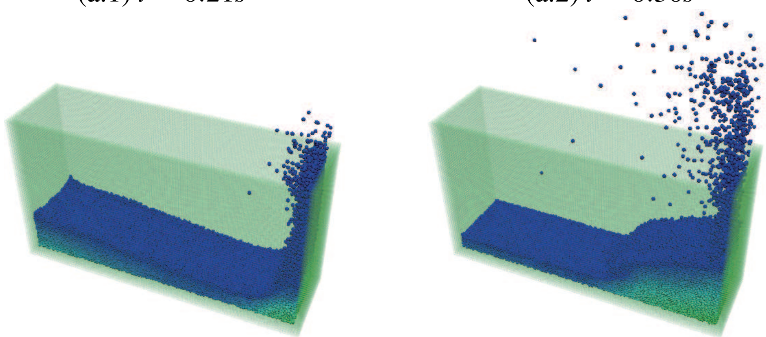

(a.3) $t \approx 0.48s$ (a.4) $t \approx 0.90s$

(a) 3D behaviors at each time on CPU-simulation

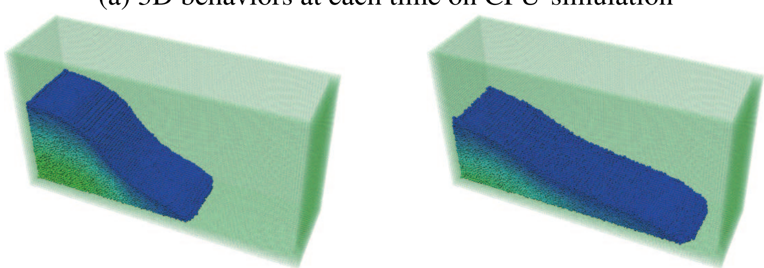

(b.1) $t \approx 0.21s$ (b.2) $t \approx 0.30s$

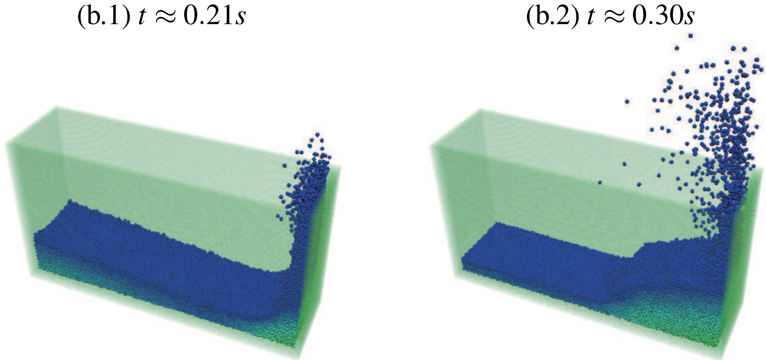

(b.3) $t \approx 0.48s$ (b.4) $t \approx 0.90s$

(b) 3D behaviors at each time on GPU-simulation

Figure 3: Particle-based simulations on CPU and GPU

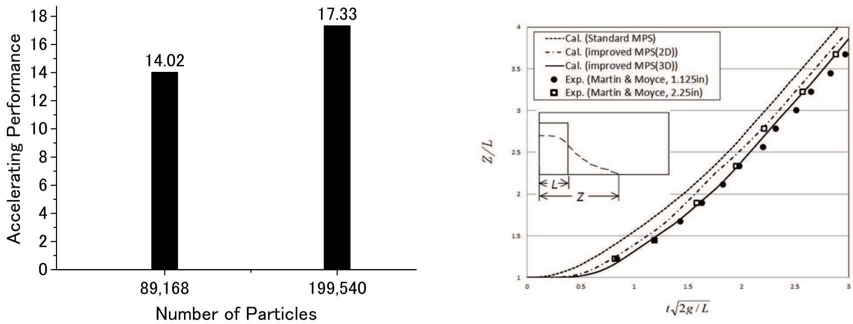

(a) GPU-accelerating performance (b) Comparisons with other data

Figure 4: GPU-accelerating performance and comparisons with experimental data

Fig. 9(c)). Our results obtained herein are qualitatively similar to the experimental photo, especially, in the left area of the impeller blades.

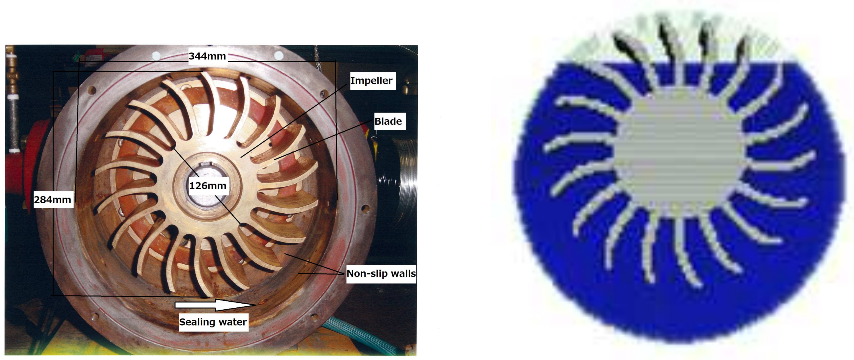

(a) Geometrical configuration (b) Initial state of particles

Figure 5: Flow in a liquid ring pump

6 Conclusions

We have presented the GPU-based MPS approach using logarithmic weighting function for solving numerically 3D incompressible viscous fluid flow problems. The standard MPS scheme has been widely utilized as a particle strategy for free surface flow, the problem of moving boundary, and multi-physics/multi-scale ones. To overcome spurious oscillations in the standard MPS method, we have proposed

(a.1) $t \approx 15ms$ (a.2) $t \approx 200ms$ (a.3) $t \approx 400ms$

(a) Particle and pressure behaviors

(b.1) $t \approx 15ms$ (b.2) $t \approx 200ms$ (b.3) $t \approx 400ms$

(b) 3D visualizations of particle and pressure behaviors

Figure 6: Particle and pressure fields at each time on GPU-simulation

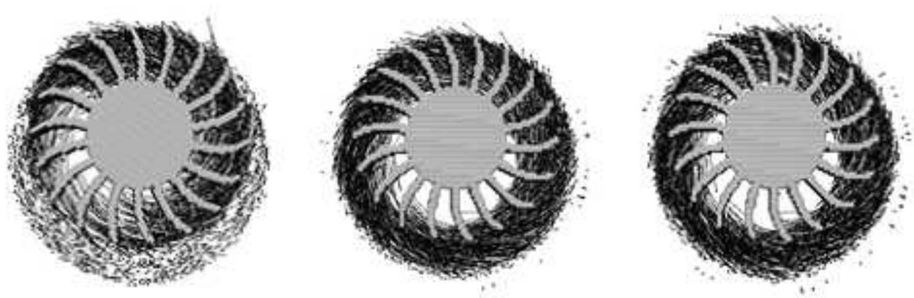

(a) $t \approx 15ms$ (b) $t \approx 200ms$ (c) $t \approx 400ms$

Figure 7: Velocity vector fields at each time on GPU-simulation

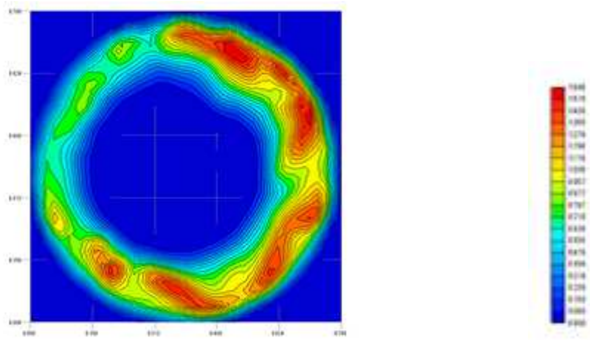

Figure 8: Time-averaged pressure fields for $t = 200 - 400ms$

(a) 2D-simulation (b) 3D GPU-simulation (c) Experiment

Figure 9: Particle behaviors and comparisons with the experimental data

to utilize the logarithmic weighting function and also take into the influence radius reduction for solving an auxiliary Poisson equation for the pressure field. The GPU implementation consists of the five steps, namely, the search for neighboring particles, the calculation of the particle number density, solving the Poisson equation with respect to the pressure fields by using GPU-based SCG method, and so forth.

As the numerical examples, the dam-breaking flow problem and the flow in a liquid ring pump with rotating impeller are carried out and compared with CPU-based particle simulation, experimental data and other numerical ones. The qualitative agreement between CPU and GPU particle-based dam-breaking flow simulations appears very satisfactory. We can see that the performance on GPU with about $200,000$ particles leads to approximately 17.33 times speedup. It is clearly confirmed that the pump forms a water ring in the impeller blades area with passage in the time.

Acknowledgement: This work was supported by Grant-in-Aid for Scientific Research (C) (KAKENHI:No.23560075) in the MEXT.

References

Amsden, A. A.; Harlow, F. H. (1970): A simplified MAC technique for incompressible fluid flow calculations. *J. Comput. Phys.*, vol.6, pp.322–325.

Atluri, S. N.; Zhu, T. (1998): A new meshless local Petrov-Galerkin (MLPG) approach in computational mechanics. *Comput. Mech.*, vol.22, pp.117–127.

Avila, R.; Atluri, S. N. (2009): Numerical solution of non-steady flows, around surfaces in spatially and temporally arbitrary motions, by using the MLPG method. *CMES: Computer Modeling in Engineering & Sciences*, vol.54, no.1, pp.15–64.

Avila, R.; Han, Z.; Atluri, S. N. (2011): A novel MLPG-finite-volume mixed method for analyzing Stokesian flows & study of a new vortex mixing flow. *CMES: Computer Modeling in Engineering & Sciences*, vol.71, no.4, pp.363–395.

Crane, K.; Llamas, I.; Tariq, S. (2008): Real-time simulation and rendering of 3d fluids. *In GPU Gems 3*, (Ed. H. Nguyen), Addison-Wesley, pp.633–675.

Du, X. H.; Shen, X. P. (2010): Numerical simulation of fluid-structure interaction of LNG prestressed storage tank under seismic influence. *CMC: Computers, Materials & Continua*, vol.20, no.3, pp.225–242.

Gingold, R. A.; Monaghan, J. J. (1977): Smoothed particle hydrodynamics: theory and application to non-spherical stars. *Mon. Not. R. astr. Soc.*, vol.181, pp.375–389.

Harada, T. (2008): Real-time rigid body simulation on GPUs. *In GPU Gems 3*, (Ed. H. Nguyen), Addison-Wesley, pp.611–632.

Harada, T.; Masaie, I.; Koshizuka, S; Kawaguchi, Y. (2008): Accelerating particle-based simulations utilizing spatial locality on the GPU. *Trans. JSCES*, (in Japanese), Paper No.20080016.

Harris, M. J. (2004): Fast fluid dynamics simulation on the GPU. *In GPU Gems*, (Ed. R. Fernando), Addison-Wesley, pp.637–665.

Hirt, C. W.; Nichols, B. D. (1981): Volume of fluid (VOF) method for the dynamics of free boundaries. *J. Comput. Phys.*, vol.39, pp.201–225.

Hori, C.; Gotoh, H.; Ikari, H; Khayyer, A. (2011): GPU-acceleration for moving particle semi-implicit method. *Computers & Fluids*, vol.51, pp.174–183.

Kakuda, K.; Ushiyama, Y; Obara, S.; Toyotani, J.; Matsuda, S.; Tanaka, H.; Katagiri, K. (2010): Flow simulations in a liquid ring pump using a particle method. *CMES: Computer Modeling in Engineering & Sciences*, vol.66, no.3, pp.215–226.

Kakuda, K.; Nagashima, T.; Hayashi, Y.; Obara, S.; Toyotani, J.; Katsurada, N.; Higuchi, S.; Matsuda, S. (2012): Particle-based fluid flow simulations on GPGPU using CUDA. *CMES: Computer Modeling in Engineering & Sciences*, vol.88, no.1, pp.17–28.

Khayyer, A.; Gotoh, H. (2009): Modified moving particle semi-implicit methods for the prediction of 2d wave impact pressure. *Coastal Engineering*, vol.56, pp.419–440.

Kondo, M.; Koshizuka, S. (2011): Improvement of stability in moving particle semi-implicit method. *Int. J. Numer. Meth. Fluids*, vol.65, pp.638–654.

Koshizuka, S.; Oka, Y. (1996): Moving-particle semi-implicit method for fragmentation of incompressible fluid. *Nucl. Sci. Eng.*, vol.123, pp.421–434.

Lin, H.; Atluri, S. N. (2001): The meshless local Petrov-Galerkin (MLPG) method for solving incompressible Navier-Stokes equations. *CMES: Computer Modeling in Engineering & Sciences*, vol.2, no.2, pp.117–142.

Lucy, L. B. (1977): A numerical approach to the testing of the fission hypothesis. *The Astronomical J.*, vol.82, no.12, pp.1013–1024.

Martin, J. C.; Moyce, W. J. (1952): An experimental study of the collapse of liquid columns on a rigid horizontal plane. *Philos. Trans. R. Soc. London Ser. A*, vol.244, pp.312–334.

Ramaswamy, B.; Kawahara, M. (1987): Lagrangian finite element analysis applied to viscous free surface fluid flow. *Int. J. Numer. Meth. Fluids*, vol.7, pp.953–984.

Stein, E; de Borst, R.; Hughes, T. J. R.. (2004): Encyclopedia of computational mechanics. *Vol.3 Fluids*, John Wiley & Sons.